

# We are IntechOpen, the world's leading publisher of Open Access books Built by scientists, for scientists

6,900

Open access books available

185,000

International authors and editors

200M

Downloads

Our authors are among the

154

Countries delivered to

TOP 1%

most cited scientists

12.2%

Contributors from top 500 universities



WEB OF SCIENCE™

Selection of our books indexed in the Book Citation Index  
in Web of Science™ Core Collection (BKCI)

Interested in publishing with us?  
Contact [book.department@intechopen.com](mailto:book.department@intechopen.com)

Numbers displayed above are based on latest data collected.  
For more information visit [www.intechopen.com](http://www.intechopen.com)



# A New Approach for Model Developing to Estimate Unmeasured Parameters in an Engine Lifetime Monitoring System

*Cristhian Maravilla and Sergiy Yepifanov*

## Abstract

Monitoring systems to predict the remaining lifetime of gas turbine engines are a major field of investigation, in particular, the monitoring systems that allow an on-line prediction. This chapter introduces and analyzes a new approach to develop mathematical models to estimate unmeasured parameters in an engine lifetime monitoring system; these models in contrast to previously developed models allow an on-line monitoring of unmeasured parameters, which are necessary to perform an on-line lifetime prediction. The blade of a high-pressure turbine (HPT) of a two-spool free turbine power plant is the test case. Several candidate models are developed for each unmeasured parameter; the best models are selected by their accuracy and robustness using the instrumental and truncation error as criteria. Ten faulty engine conditions are considered to analyze the model robustness. Two methods for model developing are compared; the first method uses physics-based models (proposed in this chapter), and the second method develops the models using the similarity concept (reference methodology). The results of the comparison show that the physics-based models are more robust to engine faults and overall they deliver a significantly more accurate prediction of the engine lifetime.

**Keywords:** gas turbine, lifetime prediction, model developing, thermodynamic relations, unmeasured parameters

## 1. Introduction

Lifetime monitoring systems are an effective way to perform condition base maintenance of gas turbine engines [1–3]; this allows a better use of the available lifetime and improvement of the engine's reliability.

Several approaches exist to predict the remaining lifetime, such as neural networks [4–7], finite element analysis (FEA) [8–10], and statistical methods [11]; however, in order to significantly enhance the accuracy of the lifetime prediction, it is necessary to estimate the lifetime in real time (on-line prediction) using actual conditions [12, 13]. All of the previously cited approaches require a large amount of computing resources, making them not suitable for an on-line application; another

limitation is that none of the cited approaches take into consideration the existing engine-to-engine differences and the performance deterioration.

Oleynik proposes in a study [14] an approach to perform on-line lifetime prediction of engine component condition (**Figure 1**); he proposes to use simple models to estimate the temperature and stresses at critical points. A major advantage of this approach is the use of actual engine operating and atmospheric conditions as input data. The methodology has been proven by practical application in monitoring of some Ukrainian engines.

As shown in **Figure 1**, one of the blocks performs the thermal condition (TC) monitoring, while the second block, the stress condition (SC) monitoring.

Inside the block of TC, it is necessary to set the thermal boundary conditions (gas temperature around the critical element and the heat transfer coefficient between the gas and metal), which are not measured parameters; the author [14] proposed a methodology to develop mathematical models based on the theory of similarity to estimate these boundary conditions.

In this chapter a new approach to develop physics-based models to estimate the unmeasured parameters is proposed and analyzed. This new approach emphasizes the accuracy of the models regardless of the engine-to-engine differences, taking into consideration a healthy and faulty engine condition.

With the help of the thermodynamic model of the engine chosen as test case, all the necessary data for model developing and validation is simulated; the simulation of the engine's component degradation is widely used in gas turbine monitoring and diagnostics [15, 16].

A comparison between the physics-based models and the reference method based on the theory of similarity proposed by [14] is conducted to validate the accuracy of the methods.

Finally, the influence of the accuracy in the prediction of the thermal boundary conditions on the errors of the engine lifetime prediction is evaluated.

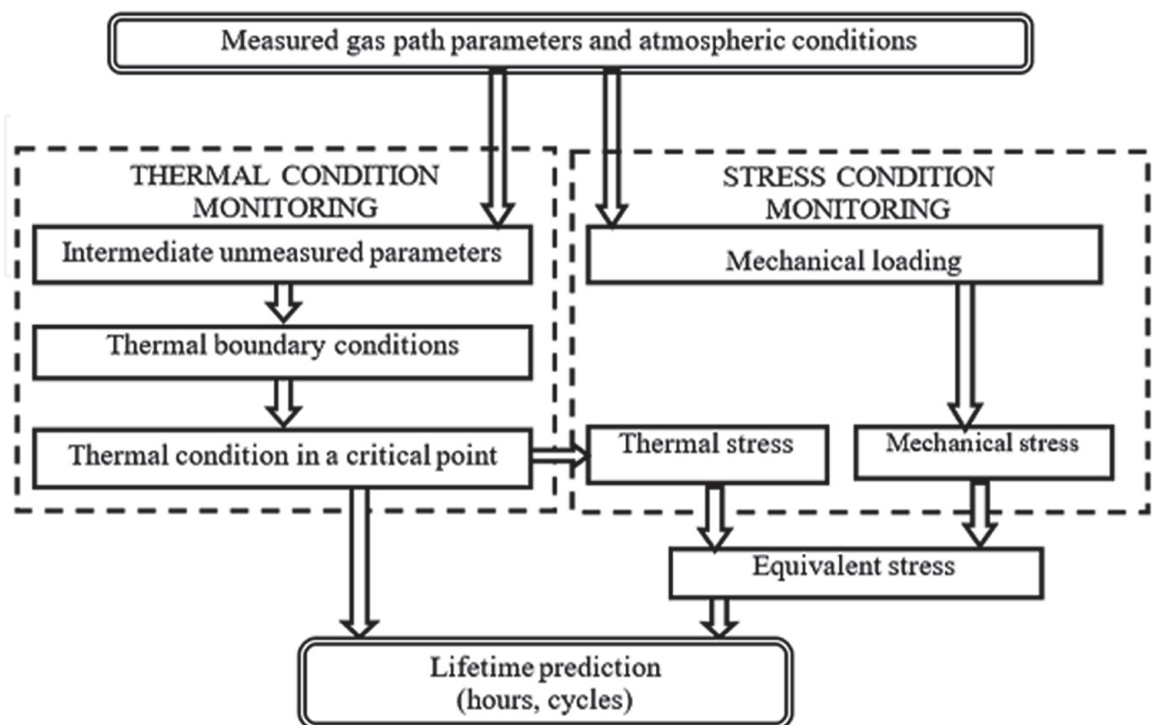


**Figure 1.**  
Scheme for on-line lifetime prediction.

## 2. Test case

It is well-known that the thermomechanical stresses in gas turbine hot elements are very high, particularly in the turbine blade having a significant effect on the safety and economics of the fleet operation [17]. For this reason, a turbine blade with three cooling channels has been chosen as the test case; the blade is mounted in the first stage of the high-pressure turbine (HPT) of a two-spool free turbine engine.

In **Table 1** the seven measured gas path parameters of the engine chosen as test case are listed.

Experience has shown that it is sufficient to consider a two-dimensional analysis of the mid-span section of the blade in order to save computing time; however, the same methodological approach can be applied for a three-dimensional geometry.

The finite element model of the mid-span turbine blade section was built with the help of FEA software. After setting all the necessary boundary conditions, the distribution of the temperature and stresses was obtained. The critical points with the smallest safety factor were found as well; as shown in **Figure 2**, the critical points correspond to the numbers 101, 102, 103, and 69.

Three critical points are located at the leading edge of the blade and one critical point at the trailing edge. For an easier analysis, the four critical points are

Designation	Gas path parameter
$G_f$	Fuel consumption
$T_C^*$	Compressor discharge temperature
$p_C^*$	Compressor discharge pressure
$T_{HPT}^*$	HPT discharge temperature
$p_{HPT}^*$	HPT discharge pressure
$T_{LPT}^*$	Low-pressure turbine (LPT) discharge temperature
$n_{HP}$	Rotational speed of the high-pressure (HP) rotor

**Table 1.**  
 List of gas path measured parameters of the engine selected as test case.

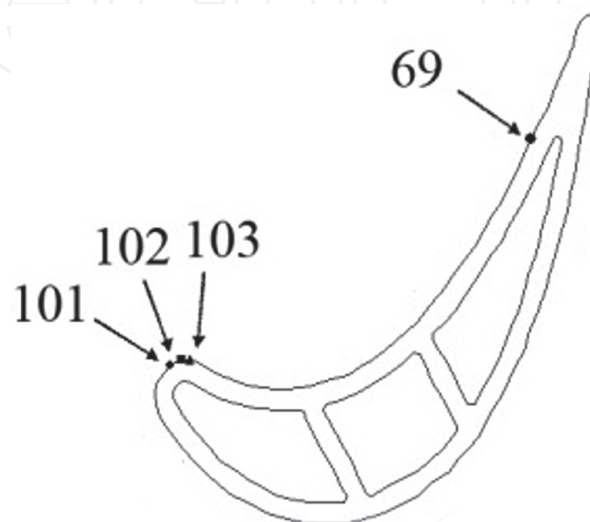


**Figure 2.**  
 Critical points at the turbine blade mid-span section.

organized into two groups: group a (GA) contains the critical points 101, 102, and 103, and group b (GB) contains the critical point number 69.

The thermodynamic model of the engine chosen as test case [18] is used to generate all the data for model developing and validation.

### 3. Engine lifetime monitoring system

A brief description of the lifetime monitoring system proposed by the author [14] is presented to have a better understanding. As shown in **Figure 1**, the block to perform the TC contains the sub-block named “thermal boundary conditions” (unmeasured parameters). The new approach for model developing proposed in this chapter focuses all the efforts in improving the accuracy in this sub-block, as improving the efficiency in the prediction of the thermal boundary conditions directly affects the accuracy of the whole monitoring system.

In the following subsection, the simple mathematical models used to estimate the blade temperature and the thermal stress at the critical points are explained.

#### 3.1 Turbine blade thermal and stress monitoring models

In [19] an analysis of the models proposed by [14] to estimate the blade temperature and stress applied to the same turbine blade and critical points was conducted. As a result, it was concluded that the best model to calculate the blade temperature at the critical points is:

$$t_{cr} = T_{S1}^* + \Theta(k_\alpha) \cdot (T_{S2}^* - T_{S1}^*) \quad (1)$$

Here  $t_{cr}$  is the blade temperature at the critical point,  $T_{S1}^*$  is the cooling temperature,  $T_{S2}^*$  is the heating temperature,  $\Theta$  is a dimensionless parameter, and  $k_\alpha$  is the relation of the heat transfer coefficients at current and reference engine operating modes:

$$k_\alpha = \alpha_i / \alpha_{ref} \quad (2)$$

Here  $\alpha_i$  and  $\alpha_{ref}$  are the heat transfer coefficients at actual and reference engine working operating modes, respectively.

The model to estimate the thermal stress at critical points is:

$$\sigma_t = \bar{S}(k_\alpha) \cdot n^2 \quad (3)$$

Here  $\sigma_t$  is the thermal stress at the critical point,  $\bar{S}$  is a dimensionless parameter, and  $n$  is the rotational speed.

The dimensionless parameters  $\Theta$  in Eq. (1) and  $\bar{S}$  in Eq. (3) are calculated as dependence of  $k_\alpha$  using a polynomial with gas path measured parameters as arguments.

The parameters  $T_{S1}^*$ ,  $T_{S2}^*$ , and  $k_\alpha$  are unmeasured parameters, which further will be referred as thermal boundary conditions; since this unmeasured parameters are the input data in Eqs. (1) and (3), it is necessary to develop mathematical models for their prediction. In the following section, the model developing methodology is explained.

#### 4. Model developing methodology

As mentioned in the introduction, a new approach for model developing is proposed. Since the models will be used in an on-line monitoring system, it is necessary to meet the following requirements:

- The models must be developed on physics-based relations, such as thermodynamic and kinematic relations and others.
- All models must use the gas path measured parameters as input data.
- The structure of the models must be simple.
- The measuring error of the gas path parameters, which are the input data of the models, must be taken into account.
- The models must have high robustness to the influence of engine's component deterioration.

Taking into account the main requirements, the following general dependence for any unmeasured parameter is proposed:

$$z = f(Y, W, T_H^*, P_H^*) \quad (4)$$

Here  $z$  is the vector of unmeasured parameters to be predicted;  $Y$  is the vector of gas path measured parameters;  $W$  is the vector of the intermediate unmeasured parameters which describe the thermodynamic properties of the fluid, such as efficiencies and pressure loss factors; and  $T_H^*, P_H^*$  are the ambient conditions.

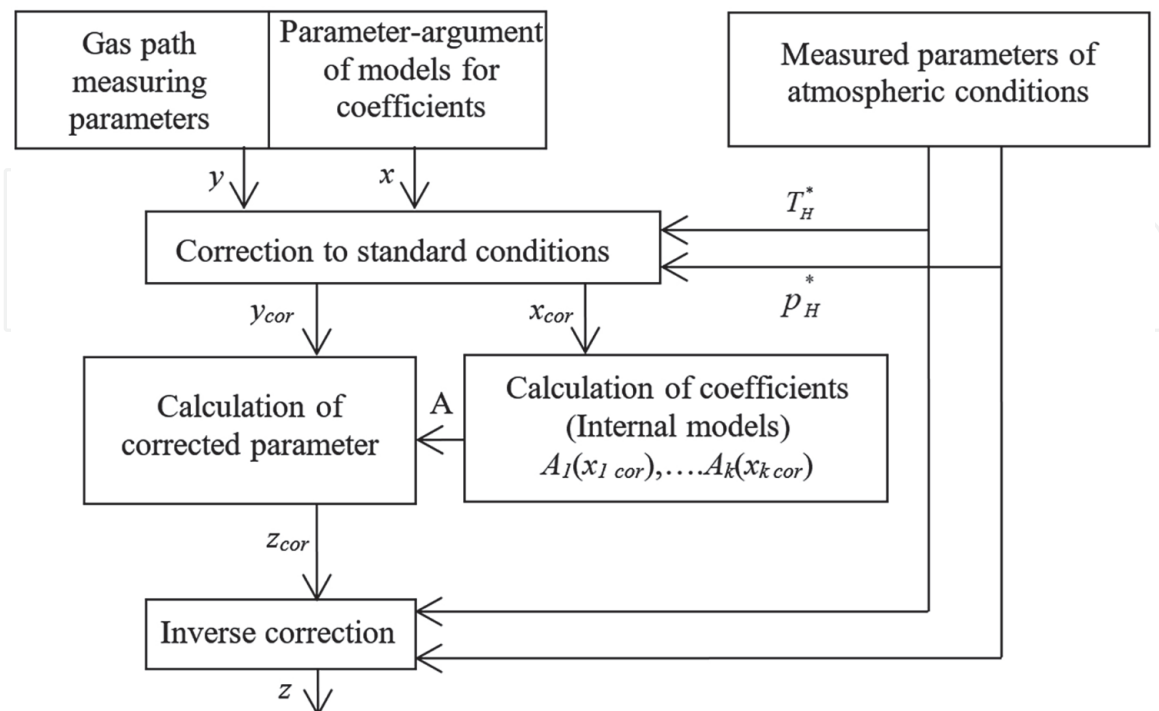


**Figure 3.**  
 Algorithm to estimate the unmeasured parameters.

As shown in Eq. (4), such dependence is not possible to be used in an on-line monitoring system since it includes the vector  $W$ , which is an unmeasured parameter. In order to solve this inconvenience, it is proposed to estimate each unmeasured parameter  $w$  as a function  $A$  (internal model) using one of the available gas path measured parameters as argument  $w = A(x)$ , where  $x$  is a gas path measured parameter.

Besides, all the parameters are corrected to standard atmosphere to take into account the influence of atmospheric conditions [20]. After rewriting Eq. (4), the general dependence for any unmeasured parameter is:

$$z_{cor} = f(Y_{cor}, A(x_{cor})) \quad (5)$$

**Figure 3** shows the algorithm to estimate the unmeasured parameters using the previously presented model developing methodology.

#### 4.1 Model verification

The best models are selected during the model verification process. The total mean square error (MSE) is the main criteria to select the best models; the MSE consists of two components, a truncation error and an instrumental error:

$$\sigma_{TT} = \sigma_{TR} + \sigma_{INS} \quad (6)$$

Here  $\sigma_{TT}$  is the total MSE,  $\sigma_{TR}$  is the truncation error, and  $\sigma_{INS}$  is the instrumental error.

##### 4.1.1 Truncation error

The mean square truncation error is:

$$\sigma_{TRj} = \sqrt{\frac{\sum_{i=1}^{N_j} (z_{j i m} - z_{j i})^2}{N_j}} \quad (7)$$

Here  $z_{j i m}$  is the value of the unmeasured parameter calculated by the developed models,  $z_{j i}$  is the true value obtained from the engine thermodynamic model, and  $N_j$  is the sample size; in other words, it is the number of engine operating points considered for analysis corresponding the engine health condition number  $j$ .

The average truncation error in percentage for any engine health conditions is obtained by:

$$\sigma_{TR m} = \frac{1}{n} \sum_{j=1}^n \sigma_{TR j} \cdot 100\% \quad (8)$$

Here  $n$  is the number of engine health conditions.

##### 4.1.2 Instrumental error

The MSE for the instrumental error for a healthy engine condition is calculated as follows:

$$\sigma_{INS} = \sqrt{\sum_{q=1}^Q \left(\frac{\partial z}{\partial y_q}\right)_i \cdot \sigma_{y_q}^2 + \sum_{K=1}^K \left(\frac{\partial z}{\partial x_K}\right)_i \cdot \sigma_{x_K}^2 + \left(\frac{\partial z}{\partial T_H^*}\right)_i \cdot \sigma_{T_H^*}^2 + \left(\frac{\partial z}{\partial p_H^*}\right)_i \cdot \sigma_{p_H^*}^2} \quad (9)$$

Here  $Q$  is the amount of gas path measured parameters, and  $K$  is the amount of internal models, which are part of the developed model to estimate the unmeasured parameterz.

The average instrumental error in percentage is obtained by:

$$\sigma_{INS\ m} = \frac{1}{N} \sum_{j=1}^n \sigma_{INS\ j} \cdot 100\% \quad (10)$$

Here  $N$  is the sample size—the number of engine operating points corresponding to a healthy engine condition.

#### 4.1.3 Model robustness analysis

Engine health conditions in real life are different from engine to engine; therefore, it is necessary to take into account these shifts from the ideal engine. For the model robustness analysis, the truncation error is calculated for several engine health conditions. In [21] the most common engine faulty conditions of a two-spool free turbine engine were analyzed; as a result, 10 faulty engine conditions were selected.

In **Table 2** the 11 engine conditions considered for analysis are listed. The deteriorated engine condition represents a 3% shift from engine health condition.

Designation	Fault parameter	Deteriorated condition
C1	—	Healthy engine
C2	$\delta\eta_C$	Compressor efficiency decrease
C3	$\delta G_C$	Compressor airflow decrease
C4	$\delta\eta_{CC}$	Combustion chamber (CC) efficiency decrease
C5	$\delta\sigma_{CC}$	Decrease in the CC total pressure
C6	$\delta\eta_{HPT}$	HPT efficiency decrease
C7	$\delta F_{NBHPT}$	HPT nozzle box (NB) area increment
C8	$\delta\sigma_{HPT-LPT}$	Decrease in the total pressure between HPT and LPT duct
C9	$\delta\eta_{LPT}$	LPT efficiency decrease
C10	$\delta F_{NBLPT}$	LPT NB area increment
C11	$\delta G_{ST}$	Increment of the air bleed for gas pumping needs

**Table 2.**  
 Engine healthy and faulty condition considered for analysis.

## 5. Developing and verification of models for unmeasured parameters for the test case

As shown in SubSection 3.1, it is necessary to calculate the input data for Eqs. (1) and (3). For our particular test case, the selected thermal boundary conditions are shown in **Table 3**.

Cooling temperature	$T_{S1}^* = T_C^*$
Heating temperature	$T_{S2}^* = T_W^*$
Relation of heat transfer coefficients for hot gases	$k_{\alpha g} = \alpha_i g / \alpha_{ref g}$
Relation of heat transfer coefficients for cooling air	$k_{\alpha a} = \alpha_i a / \alpha_{ref a}$

Here  $T_C^*$  is the compressor discharge temperature, and  $T_W^*$  is the gas temperature in relative motion in front of the first turbine stage.

**Table 3.**  
Thermal boundary conditions for our test case.

It is necessary to develop alternative models for each one of the selected thermal boundary conditions. Although the compressor discharge temperature is a measured gas path parameter for our test case (**Table 1**), it is of particular interest to analyze the effect of its inclusion or exclusion from the list of gas path measured parameters in the overall lifetime prediction.

Since many alternative models were developed, only one example will be shown in order to save available text space; for more details consult [21].

### 5.1 Model developing

Let us consider the gas temperature at the inlet of the turbine  $T_g^*$ . As mentioned in Section 4, the models must be physics-based; therefore, we use the relation that describes the power balance between the high-pressure turbine and the high-pressure compressor [20] as the base equation for model developing:

$$N_T \cdot \eta_m = N_C \quad (11)$$

Here  $N_T$  is the turbine power,  $\eta_m$  is the mechanical efficiency, and  $N_C$  is the compressor power.

Let us take into account that:

$$N_T = G_g \cdot L_T = G_g \cdot C_{p g} \cdot (T_g^* - T_T^*) \quad (12)$$

$$N_C = G_a \cdot L_C = G_a \cdot C_{p a} \cdot (T_C^* - T_H^*) \quad (13)$$

Here  $G_g$  and  $G_a$  are the gas and air flow consumptions accordingly, and  $C_{p g}$  and  $C_{p a}$  are the specific heat values at constant pressure for gas and air accordingly.

Solving Eq. (11) for  $T_g^*$ , we obtain:

$$T_g^* = \left( \frac{C_{p a}}{C_{p g}} \cdot \frac{G_a}{G_g \cdot \eta_m} \right) \cdot (T_C^* - T_H^*) + T_{HPT}^* \quad (14)$$

All the unmeasured parameters in Eq. (14) will be described with the help of the internal model  $A_{TG1}$ :

$$A_{TG1} = \left( \frac{C_{p a}}{C_{p g}} \cdot \frac{G_a}{G_g \cdot \eta_m} \right) \quad (15)$$

Let us remember that all the internal models will be calculated as a polynomial functions using one of the available gas path measured parameters as argument.

Finally, after making the correction to standard atmospheric conditions of Eq. (14), we arrive at the following expression:

$$T_{g\text{ cor}}^* = A_{TG1\text{ cor}}(x) \cdot (T_{C\text{ cor}}^* - T_0) + T_{HPT\text{ cor}}^* \quad (16)$$

Here  $T_0 = 288.15$  K is the value of standard atmospheric temperature.

Several models can be developed for the same unmeasured parameter based on different source equations (alternative models). **Figure 4** shows the general scheme for the developing of alternative models.

Using the scheme shown in **Figure 4**, a total of 31 models were developed for our test case (see reference [21]). A name is given to each developed model for easier identification, for example, the model shown in Eq. (16) is named MTG1. The names and arguments for each alternative developed model are shown in **Figure 5**.

## 5.2 Model verification

Let us consider the model MTG1 shown in Eq. (16), which includes the internal model  $A_{TG1\text{ cor}}(x)$ . It is necessary to analyze which of the gas path measured parameters (**Table 1**) is best suited to be used as argument in the polynomial, as well as the degree of the polynomial that results in the most accurate prediction of  $T_g^*$ .

All of the necessary data for the analysis was obtained using the thermodynamic model of the engine selected as test case [18]. A total of 245 engine operating modes for a healthy engine condition were simulated; these operating modes describe the whole range of the engine operating conditions.

The generated data was randomly divided into two sets. The first set of 123 operating points is used as reference. The second set of 122 operation modes is for model validation. Using the data from the reference set, the coefficients for the polynomial functions were obtained using the least square method.

The polynomial degree was changed from 1 to 4 using each one of the gas path measured parameters (see **Table 1**) as argument in the polynomial.

Once all the polynomial coefficients describing the internal model  $A_{TG1\text{ cor}}(x)$  were obtained, the value of  $T_g^*$  was calculated. According to the scheme shown in

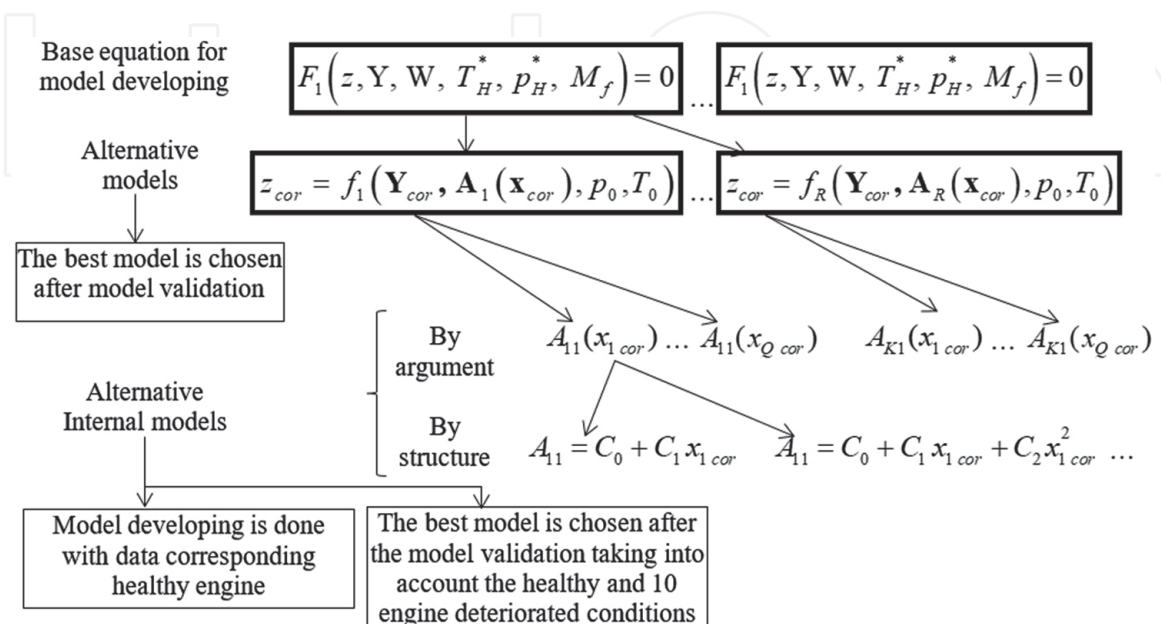


**Figure 4.**  
 Scheme for the developing the alternative models.

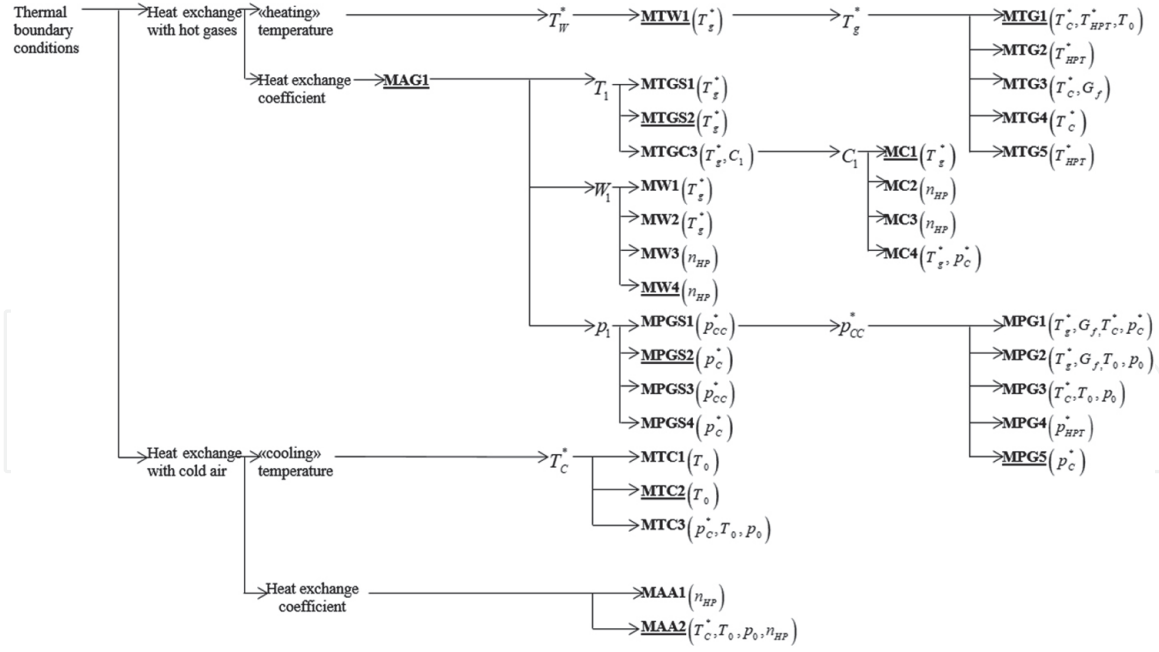


**Figure 5.**  
Structure of the alternative models developed for our test case.

**Figure 3**, it is necessary to perform an inverse conversion of Eq. (16) to calculate the value of  $T_g^*$  as follows:

$$T_g^* = [A_{TG1\ cor}(x) \cdot (T_{C\ cor}^* - T_0) + T_{HPT\ cor}^*] \cdot \frac{T_H^*}{T_0} \quad (17)$$

The total error (see Eq. (6)) was the main criteria to assess the accuracy of the developed models. A total of 11 engine conditions (**Table 2**) were considered for the model validation (model robustness analysis).

**Figure 6(a)** depicts the total error in the prediction of  $T_g^*$  using the model  $\underline{MTG1}$  with different gas path measured parameters as argument in the polynomial to describe the internal model  $A_{TG1\ cor}(x)$ . From this figure it is clear that the lowest error is obtained when  $T_{HPT}^*$  is set as argument.

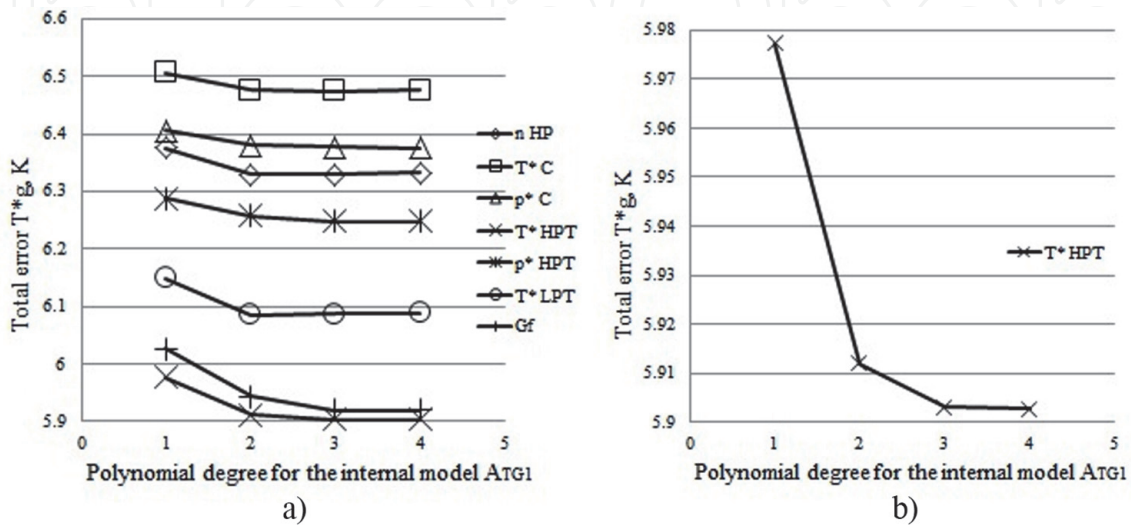


**Figure 6.**  
Total error in the prediction of  $T_g^*$  using model  $\underline{MTG1}$ . (a) Using seven different measured parameters as argument; (b) detailed view for the best argument.

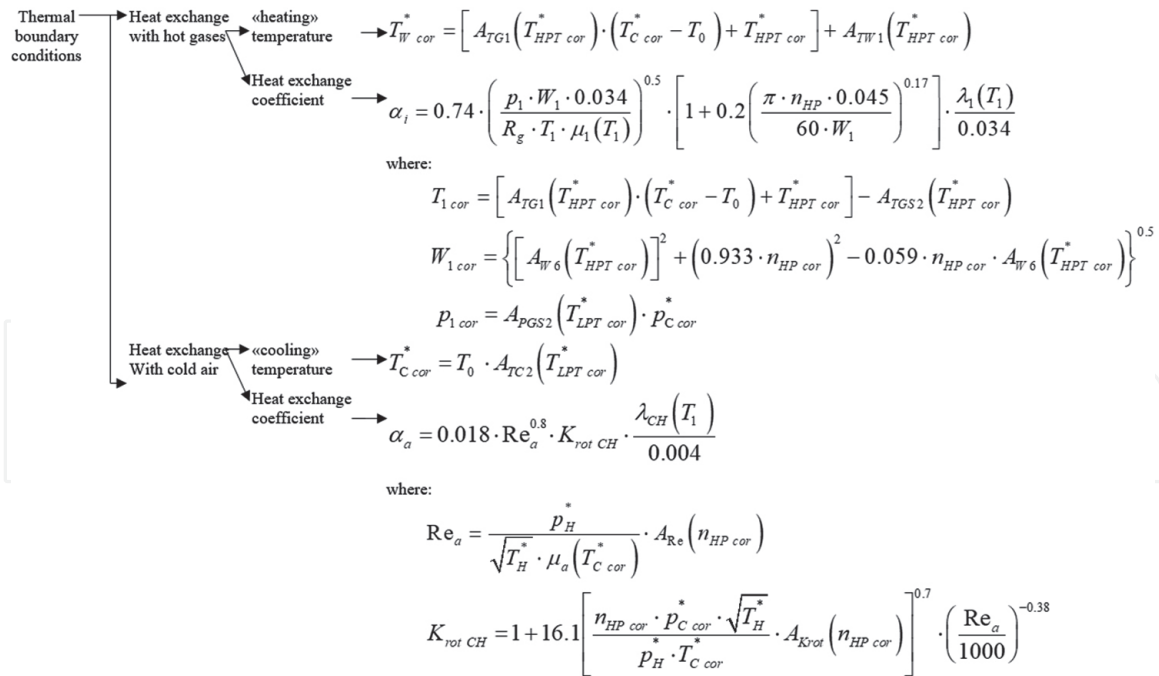


**Figure 7.**  
 Selected models to monitor the thermal boundary conditions of the test case.

**Figure 6(b)** shows that it is sufficient to use a third-degree polynomial as further increment does not reduce the total error in the prediction.

From this analysis the polynomial degree and the gas path measured parameter to be used as argument in Eq. (17) are selected:

$$A_{TG1\text{ cor}}(x) = (-6.79 \cdot 10^{-10} \cdot T_{HPT\text{ cor}}^{*3} + 2.19 \cdot 10^{-6} \cdot T_{HPT\text{ cor}}^{*2} - 2.47 \cdot 10^{-7} \cdot T_{HPT\text{ cor}}^* + 1.87) \quad (18)$$

The selection of the argument in the *i*-internal models and the best polynomial degree for all the developed models was done using the same methodology. After the model verification of all the developed models, the best models were selected. **Figure 7** shows the selected models to calculate the thermal boundary conditions for the test case.

## 6. Comparative analysis for the model accuracy

Let us conduct a comparative analysis between two approaches for model developing: the first approach for model developing [14] uses the theory of similarity (reference model), and the second approach is proposed in this chapter and uses a physics-based methodology.

### 6.1 Thermal boundary condition prediction

The thermal boundary conditions for our test case (see **Table 3**) were calculated using models developed with both methodologies.

The total error was calculated according to Eq. (6), and the model robustness analysis took into account the 11 engine health conditions listed in **Table 2**. It is of particular interest to analyze the model robustness, since such analysis for the reference methodology does not exist.

In **Figure 8** the truncation errors for the thermal boundary condition prediction are presented.

From **Figure 8**, it is clear that the models developed using the approach introduced in this chapter are more robust; it means that the models are less sensitive to the deviations from a healthy engine condition. This is a major advantage compared to the reference methodology based in the theory of similarity [14].

## 6.2 Prediction of the thermal-stress condition and engine lifetime

The thermal-stress engine condition was calculated using Eqs. (1) and (2). The prediction of the turbine blade lifetime is a very complex process, which involves different factors; however, a conservative lifetime prediction will be enough to assess the impact that a new model developing methodology has on the accuracy of the lifetime prediction. According to the author [22], a practical way to predict lifetime is the Larson-Miller relation:

$$t_r = 10^{PLM/t_{cr}-C} \quad (19)$$

Here  $PLM$  is the Larson-Muller parameter;  $C$  is a coefficient, which for the test case is equal to 20.

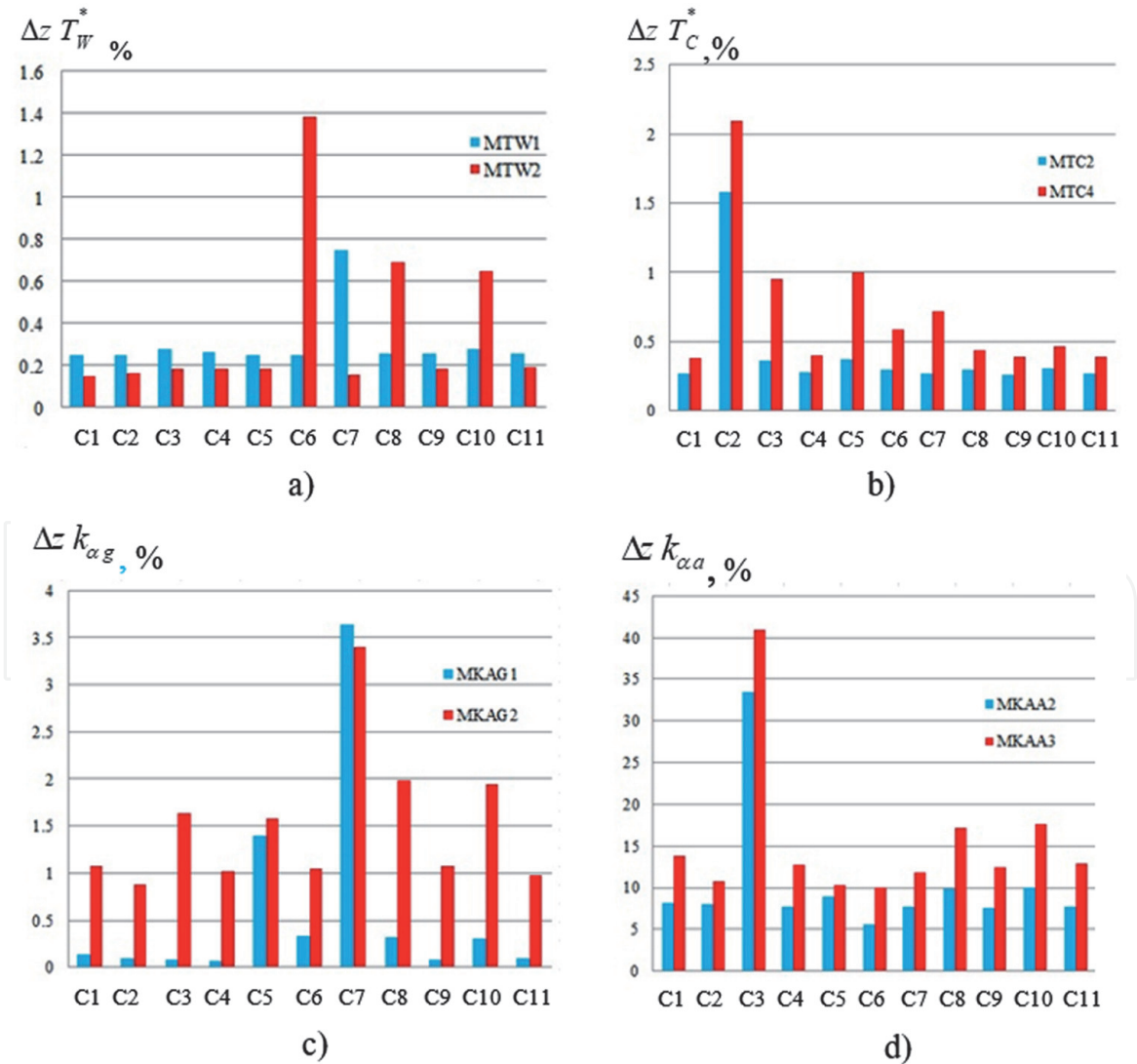


**Figure 8.**

Truncation error in the prediction of thermal boundary conditions for different engine health conditions. Blue color, physics-based models; red color, models developed on theory of similarity. (a)  $T_W^*$ ; (b)  $T_C^*$ ; (c)  $k_{\alpha g}$ ; (d)  $k_{\alpha a}$ .

As mentioned in Section 5, it is of particular interest to analyze what is the influence of the inclusion or exclusion of the compressor temperature  $T_C^*$  as a gas path measured parameter in the accuracy of TC, SC, and lifetime prediction  $t_r$ . Therefore, the thermal-stress condition and lifetime prediction are calculated for two cases. For the first case, the compressor temperature is not measured, and for the second case, the compressor temperature is measured.

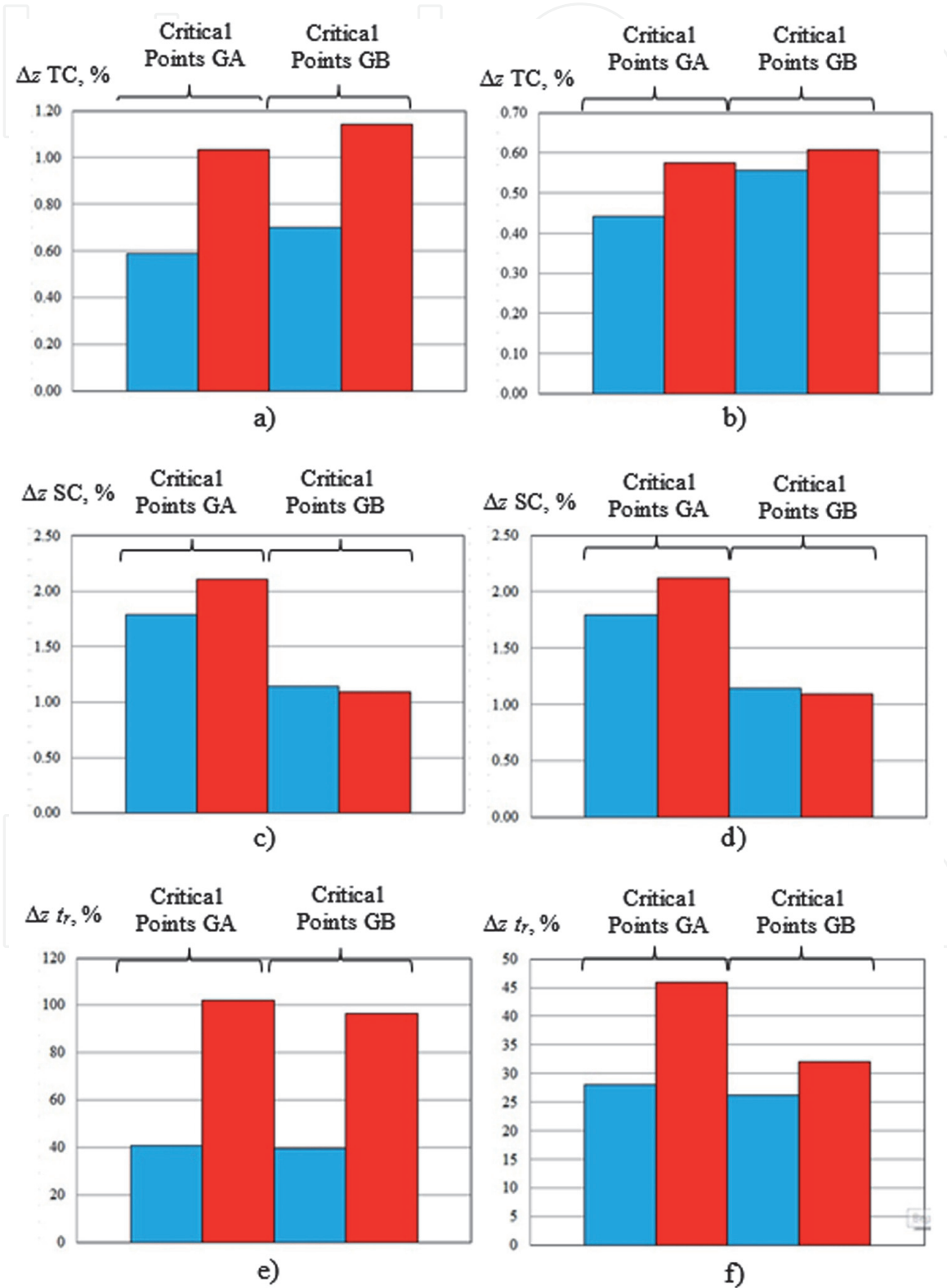


**Figure 9.** Total error in the prediction of TC, SC, and  $t_r$ . Blue color, physics-based models; red color, models developed on the theory of similarity. (a, c, e)  $T_C^*$  is an unmeasured parameter; (b, d, f)  $T_C^*$  is a measured parameter.

### 6.2.1 Prediction of the thermal-stress condition and engine lifetime when the compressor temperature is not measured

**Figure 9** presents the total error in the prediction of TC, SC, and lifetime  $t_r$ . From **Figure 9(a)** it is clear that the physics-based models give a better prediction of TC. **Figure 9(c)** shows that the improvement in the prediction of SC is not as significant, especially for the critical points GB. **Figure 9(e)** shows that the prediction of the lifetime  $t_r$  is highly improved compared to the results obtained when the models based on the theory of similarity are used to calculate the thermal boundary conditions.

From this analysis, it is clear that the methodology used for developing the models of the unmeasured parameters has a great impact in the final accuracy of the lifetime  $t_r$  prediction.

### 6.2.2 Prediction of the thermal-stress condition and engine lifetime when the compressor temperature is measured

We repeated the calculation, but this time the value of the compressor temperature is measured. **Figure 9(b)** shows that the total error in the prediction of TC for both groups is still better when using physics-based models.

**Figure 9(d)** shows that the accuracy in the prediction of the SC is not significantly affected. From **Figure 9(f)** it is clear that the improvement in the prediction of TC has a significant impact in the prediction of the lifetime  $t_r$ , for example, for the critical point GA when using physics-based models, an improvement in the prediction of TC from 0.58 to 0.44% leads to a better lifetime prediction from 45.95 to 27.96%.

We can conclude that the accuracy in the prediction of the lifetime is highly improved when the temperature after the compressor is a measured parameter.

## 7. Conclusions

A new approach for model developing to estimate the unmeasured parameters in an engine lifetime monitoring system was introduced. This is an effort to increase the accuracy of the lifetime prediction.

All the developed models have a very simple structure and are physics-based, making them ideal to be applied in an on-line lifetime monitoring system.

A turbine blade mounted on the first stage of the high-pressure turbine of a two-spool free turbine power plant is the test case.

Several alternative models were developed using different basic equations. Some of the models include in their structure an internal model, which characterizes the thermodynamic properties of the working fluid, such as efficiencies, pressure loss factors, and others. The internal models were defined by a polynomial function. The best measured parameter used as argument in the polynomial and the degree of the polynomial function were selected using the mean square error as criteria.

All the necessary data for model developing and validation was generated with the engine thermodynamic model.

The truncation and instrumental error are the main criteria to select the best models. Ten engine faulty conditions were considered for the robustness analysis of the models.

A comparative analysis between two model developing methodologies was conducted: physics-based methodology (proposed in this chapter) and models developed on the theory of similarity (reference). The results show that the physics-based models are less sensitive to shifts from the engine healthy condition.

It was found that the use of the proposed model developing methodology provides a better estimation of the thermal boundary conditions, which leads to a significantly better prediction of the lifetime.

It was proven that the compressor temperature has a great impact in the lifetime prediction. If this parameter is not measured, then the accuracy of the lifetime prediction is significantly worse compared to the results obtained when the compressor temperature is measured.

The obtained results show that it is possible to use the proposed model developing methodology in real applications; however, it is necessary to take into account a proper interpretation of the results obtained in this chapter. The reference data, which was used to determine the accuracy of the models, is simulated data; therefore, it is possible that the errors of the lifetime monitoring under real conditions will grow. To avoid such inconvenience, it is possible to replace the data generated with the help of the engine thermodynamic model with real data. This approach is valid, since the engine thermodynamic model is not part of the proposed model developing methodology. In order to obtain the necessary real data, it will be necessary to use additional instrumentation under engine test bed conditions.

## Nomenclature

### Subscripts

<i>a</i>	air
<i>cor</i>	corrected parameter
<i>cr</i>	critical point
<i>C</i>	compressor
<i>CC</i>	combustion chamber
<i>CH</i>	channel
<i>f</i>	fuel
<i>g</i>	gas
<i>H</i>	atmospheric conditions
<i>HP</i>	high pressure
<i>HPT</i>	high-pressure turbine
<i>i</i>	i-engine mode
<i>INS</i>	instrumental error
<i>j</i>	j-engine health condition
<i>LPT</i>	low-pressure turbine
<i>m</i>	value calculated with the help of models, mechanical
<i>NB</i>	nozzle box
<i>ref</i>	reference engine mode
<i>ST</i>	gas pumping station
<i>S1</i>	cooling
<i>S2</i>	heating
<i>t</i>	thermal
<i>T</i>	turbine
<i>TR</i>	truncation error
<i>TT</i>	total mean square error
<i>W</i>	relative velocity

## Designations

G	consumption
T	temperature
p	pressure
n	rotational speed, number of engine health conditions
t	blade temperature
k	coefficient, isentropic factor
$\bar{S}$	dimensionless parameter
z	unmeasured parameter
Y	gas path measured parameters
W	unmeasured parameters describing thermodynamic properties of the working fluid
A	internal model
x	measured parameter, argument of polynomial
$p_0$	standard atmospheric pressure (101.3 KPa)
$T_0$	standard atmospheric temperature (288.15 K)
y	measured parameter
N	sample size (number of engine operation modes), power
C	engine condition, coefficient
L	thermodynamic work
$C_p$	specific heat at constant pressure
A	coefficient
Re	Reynolds number
$K_\alpha$	relation of heat transfer coefficient at current and at a reference operation mode
$t_r$	lifetime

## Greek symbols

*	stagnation parameter
$\alpha$	heat transfer coefficient
$\Theta$	dimensionless parameter
$\sigma$	stress, mean square error, total pressure conservation
$\eta$	efficiency
$\delta$	shift from healthy engine condition
$\mu$	dynamic viscosity

## Author details

Cristhian Maravilla\* and Sergiy Yepifanov  
National Aerospace University of Ukraine, Kharkiv, Ukraine

\*Address all correspondence to: [cris\\_mahe@hotmail.com](mailto:cris_mahe@hotmail.com)

## IntechOpen

© 2019 The Author(s). Licensee IntechOpen. This chapter is distributed under the terms of the Creative Commons Attribution License (<http://creativecommons.org/licenses/by/3.0>), which permits unrestricted use, distribution, and reproduction in any medium, provided the original work is properly cited. 

## References

- [1] Jin H, Lodwen P, Pistor R. Remaining life assessment of power turbine disks. In: Proceedings of ASME Turbo Expo 2008: Power for Land, Sea and Air. Berlin, Germany: GT2008-51010; 2008
- [2] Alexander V. Gas turbine plant thermal performance degradation assessment. In: Proceedings of ASME Turbo Expo 2008: Power for Land, Sea and Air. Berlin, Germany: GT2008-50032; 2008
- [3] Phillip D, David D. Remaining life assessment technology applied to steam turbines and hot gas expanders. In: Proceedings of ASME Turbo Expo 2011: Power for Land, Sea and Air. Vancouver, Canada: GT2011-45324; 2011
- [4] Parthasarathy G, Menon S, Richardson K. Neural network models for usage based remaining life computation. In: Proceedings of ASME Turbo Expo 2006: Power for Land, Sea and Air. Barcelona, Spain: GT2006-91099; 2006
- [5] Yoon J, Kim T, Lee J. Simulation of performance deterioration of a microturbine and application of neural network to its performance diagnosis. In: Proceedings of ASME Turbo Expo 2008: Power for Land, Sea and Air. Berlin, Germany: GT2008-51494; 2008
- [6] Fast M, Assadi M, De S. Condition based maintenance of gas turbines using simulation data and artificial neural networks: A demonstration of feasibility. In: Proceedings of ASME Turbo Expo 2008: Power for Land, Sea and Air. Berlin, Germany: GT2008-50768; 2008
- [7] Palme T, Breuhaus P, Assadi M. Early warning of gas turbine failure by nonlinear feature extraction using an auto-associative neural network approach. In: Proceedings of ASME Turbo Expo 2011: Power for Land, Sea and Air. Vancouver, Canada: GT2011-45991; 2011
- [8] Blumenthal R, Hutchinson B, Zori L. Investigation of transient CFD methods applied to a transonic compressor stage. In: Proceedings of ASME Turbo Expo 2011: Power for Land, Sea and Air. Vancouver, Canada: GT2011-46635; 2011
- [9] Weiss J, Subramanian V, Hall K. Simulation of unsteady turbomachinery flows using an implicitly coupled nonlinear harmonic balance method. In: Proceedings of ASME Turbo Expo 2011: Power for Land, Sea and Air. Vancouver, Canada: GT2011-46367; 2011
- [10] Jeromin A, Eichler C, Noll B. Full 3D conjugate heat transfer simulation and heat transfer coefficient prediction for the effusion-cooled warm of a gas turbine combustor. In: Proceedings of ASME Turbo Expo 2008: Power for Land, Sea and Air. Berlin, Germany: GT2008-50422; 2008
- [11] Giuseppe F, Carlevaro F. Gas turbine maintenance policy: A statistical methodology to prove interdependency between number of starts and running hours. In: Proceedings of ASME Turbo Expo 2002: Power for Land, Sea and Air. Amsterdam, Netherlands: GT2002-30281; 2002
- [12] Eshati S, Abdul Ghafir M, Laskaridis P, Li Y. Impact of operating conditions and design parameters on gas turbine hot section creep life. In: Proceedings of ASME Turbo Expo 2010: Power for Land, Sea and Air. Glasgow, UK: GT2010-22334; 2010
- [13] Maccio M, Rebizzo A, Traversone L, Bordo L. Rotor components life evaluation validated by field operation data. In: Proceedings of ASME Turbo

- Expo 2010: Power for Land, Sea and Air. Glasgow, UK: GT2010-22741; 2010
- [14] Oleynik A. Concepts and development of methods for lifetime monitoring based on the identification of the dynamics of the thermal-stress conditions of aviation GTE critical components [thesis]. National Aerospace University of Ukraine; 2006
- [15] Jiang L, Eli H, Hee-Koo M. 3D rams prediction of gas-side heat transfer coefficients on turbine blade and end wall. In: Proceedings of ASME Turbo Expo 2011: Power for Land, Sea and Air. Vancouver, Canada: GT2011-46723; 2011
- [16] Abubakar M, Reyad A, Gordon E, John E. Conjugate heat transfer CFD predictions of impingement heat transfer: Influence of the number of holes for a constant pitch to diameter ratio X/D. In: Proceedings of ASME Turbo Expo 2014: Power for Land, Sea and Air. Dusseldorf, Germany: GT2014-25268; 2014
- [17] Wieslaw B, Zhong Z, David D, Chen W, Wu X. Residual life assessment of a critical component of a gas turbine – Achievements and challenges. In: Proceedings of ASME Turbo Expo 2014: Power for Land, Sea and Air. Dusseldorf, Germany: GT2014-26423; 2014
- [18] Yepifanov S, Kuzmenko B, Ryumshin N. Synthesis of Turbine Engine Control and Diagnosing Systems. Kiev, Ukraine: Technical Publishing; 1998
- [19] Maravilla C, Yepifanov S, Loboda I. Improved turbine blade lifetime prediction. In: Proceedings of ASME Turbo Expo 2015: Power for Land, Sea and Air. Montreal, Canada: GT2015-43046; 2015
- [20] Kulagin B. Theory and Design of Aircraft Engines and Power Plants. Moscow: Mashinostroenie; 2003. p. 616
- [21] Maravilla C. Improvement in the prediction of the thermal boundary conditions in a turbine blade monitoring system [thesis]. National Aerospace University of Ukraine; 2016
- [22] Krykonov D. Handbook of Engine Lifetime Prediction. Kharkiv, Ukraine: National Aerospace University of Ukraine; 2005. p. 67